

ALMOST CYLINDRICAL ISOROTATING LIQUID BRIDGES FOR SMALL BOND NUMBERS

J.M. Vega & J.M. Perales

ETSI, Aeronáuticos, Universidad Politécnica de Madrid, Spain

ABSTRACT

In the absence of gravity, a cylindrical-shaped liquid bridge becomes unstable as the slenderness of the bridge Λ exceeds a critical value Λ_c , which depends on the rotational Weber number W . The unstable mode is either axisymmetric (amphora-mode) or non-axisymmetric (C-mode) depending on whether W is smaller or bigger than $1/3$.

Almost cylindrical bifurcating stationary shapes, with a cylindrical volume, are calculated for $|\Lambda - \Lambda_c| \ll 1$. It is seen that the bifurcation is always subcritical, i.e., the bifurcating non-cylindrical shapes appear for $\Lambda < \Lambda_c$.

The effect of a small axial gravity, i.e., a small gravitational Bond number B is also considered. It is seen that $\Lambda_c(0, \Lambda) - \Lambda_c(B, \Lambda)$ is of the order of $B^{2/3}$ for amphora modes, and of the order of B^2 for C-modes.

Finally, a comparison is made with numerical and experimental results available in the Literature, and some comments on the dynamical behaviour of the liquid bridge are given.

Keywords: Floating zone, Liquid bridge, Microgravity, Interfaces, Bifurcation.

1. INTRODUCTION

It is well known (Refs. 1-4) that, in the absence of gravity, a cylindrical-shaped rotating liquid bridge, bounded by two coaxial end discs (see Figure 1), becomes unstable if the slenderness of the bridge Λ ($\Lambda = L/2R$ where L is the distance between the discs and R is their radius) satisfies

$$\Lambda > \Lambda_c \equiv \begin{cases} \pi/\sqrt{1+W} & \text{if } W \leq 1/3 \\ \pi/\sqrt{4W} & \text{if } W > 1/3 \end{cases}$$

i.e., if the point (Λ, W) is above the curve ABC in Figure 2. The Weber number W is defined as $W = \rho \Omega^2 R^3 / \sigma$, where ρ is the density of the liquid, σ is its surface tension coefficient and Ω is the angular velocity.

Local bifurcation Theory will be used, in sections 2-3, to obtain an asymptotic description, as $\Lambda \rightarrow \Lambda_c$,

of the bifurcating noncylindrical shapes. For numerical computations see Ref. 5, where an asymptotic analysis, as $\Lambda \rightarrow \Lambda_c$, of the (axisymmetric) case $W \leq 1/3$ may also be found.

The effect of a small axial gravity g , which is measured by the gravitational Bond number $B = \rho g R^2 / \sigma$, will be considered in section 4. A typical value of $\sigma / \rho R^2$ is 5 cm/sc^2 ($R = 4 \text{ cm}$, water); therefore, the gravitational effect should not be ignored even for extremely small values of g (say, $5 \cdot 10^{-4}$ times its value at the surface of the Earth).

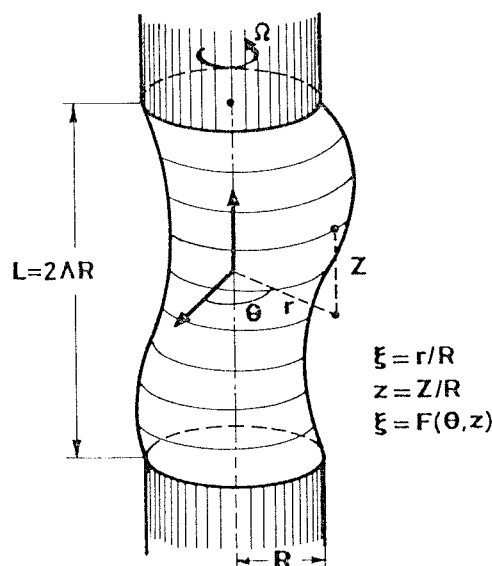


Figure 1. Sketch of the liquid bridge.

1.1 Equilibrium equation

The equation governing the steady shape of the liquid bridge is obtained by expressing the equilibrium between surface tension and local pressure forces at the free surface of the liquid. After suitable non-dimensionalization, it may be written as

$$M(F) + p + \frac{1}{2} W F^2 - Bz = 0 \quad (1)$$

where $\xi = F(\theta, z)$ is the equation of the free surface in cylindrical coordinates (see Figure 1), p is the (nondimensional) pressure at $\xi = z = 0$, and the local mean curvature $M(F)$ is (Ref. 6),

$$M(F) = \frac{F(1+F_z^2)(F_{\theta\theta}-F)+FF_{zz}(F^2+F_\theta^2)-2F_\theta(F_\theta+FF_zF_{\theta z})}{[F^2(1+F_z^2)+F_\theta^2]^{3/2}} \quad (2)$$

Equation 1 is to be integrated with the boundary conditions

$$F(\theta, \pm A) = 1 \ ; \ F(\theta+2\pi, z) \equiv F(\theta, z) \quad (3)$$

(liquid bridge anchored to the edges of the end discs, azimuthal periodicity), and the condition of conservation of the volume of the bridge,

$$\left| \int_{-A}^A dz \int_0^{2\pi} r^2 d\theta \right| = 4\pi A \quad (4)$$

1.2 Linear stability in the absence of gravity
($B=0$)

Let us look for solution of Eqs. 1-4 of the form

$$F = F_e + \epsilon \bar{F} + o(\epsilon) \ , \quad p = p_e + \epsilon \bar{p} + o(\epsilon)$$

where $F_e \equiv 1$, $p_e = 1 - W/2$ (cylindrical liquid bridge) and $\epsilon \ll 1$. \bar{F} and \bar{p} are seen to be given by the linear problem

$$\bar{F}_{zz} + \bar{F}_{\theta\theta} + (1+W)\bar{F} + \bar{p} = 0 \quad (5)$$

$$\bar{F}(\theta, \pm A) = 0 \ , \ \bar{F}(\theta+2\pi, z) \equiv \bar{F}(\theta, z) \ , \ \int_{-A}^A dz \int_0^{2\pi} \bar{F} d\theta = 0 \quad (6)$$

which has the nontrivial solutions:

Axisymmetric:

- If $A\sqrt{1+W} = j\pi \ (j = 1, 2, \dots)$,

$$\bar{F}(\theta, z) = \sin(\sqrt{1+W}z) \ , \ \bar{p} = 0 \ .$$

- If $A\sqrt{1+W} = \lambda_k \ (\tan \lambda_k = \lambda_k, \ k = 1, 2, \dots)$

$$\bar{F}(\theta, z) = \frac{\bar{p}}{\sqrt{1+W}} \left[1 - \frac{\cos(\sqrt{1+W}z)}{\cos(\sqrt{1+W}A)} \right]$$

Non-axisymmetric:

- If $A\sqrt{1+W-n^2} = m\pi/2 \ (n, m = 1, 2, \dots)$

$$\bar{F}(\theta, z) = \cos n\theta \sin(\sqrt{1+W-n^2}z + m\pi/2) \ , \ \bar{p} = 0$$

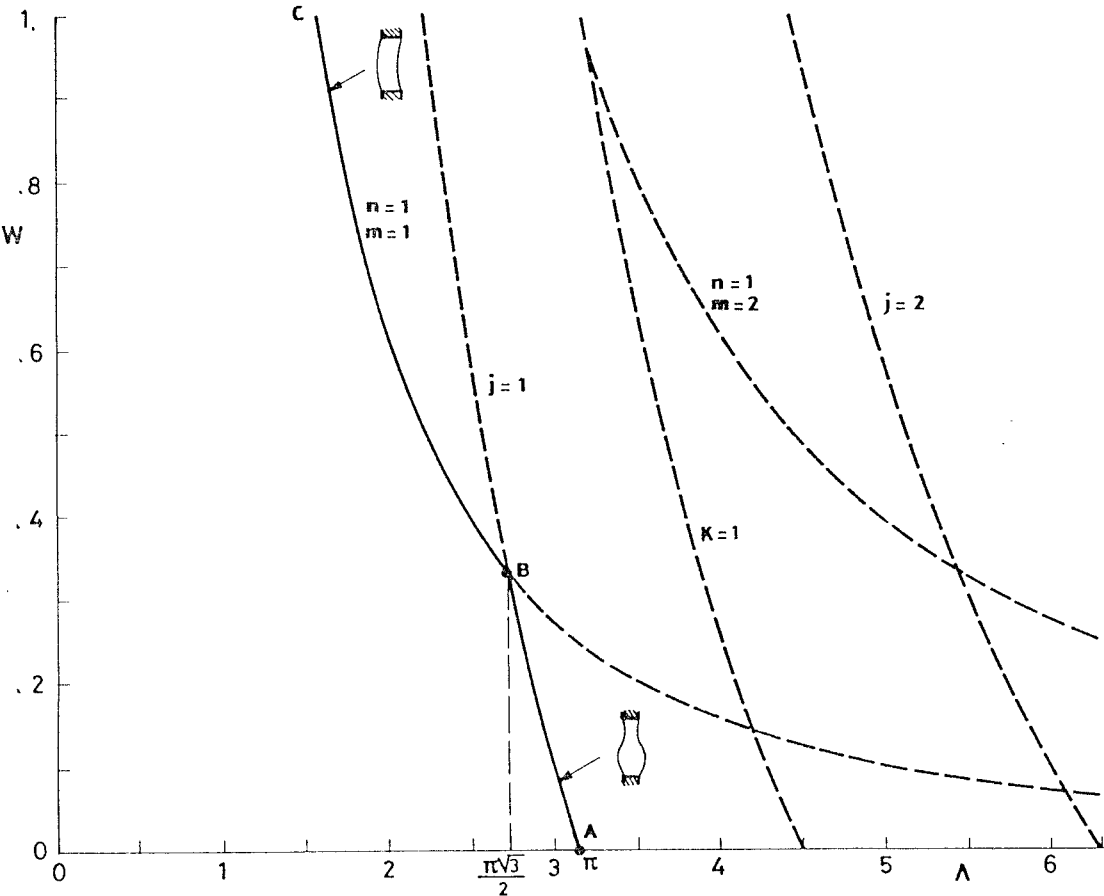


Figure 2. Stability diagram (no gravity).

Bifurcation (from cylinders) to noncylindrical equilibrium shapes appears only (Implicit Function Theorem, Ref. 7) near the curves $\Lambda\sqrt{1+W} = k\pi$, $\Lambda\sqrt{1+W} = \lambda_k$, $\Lambda\sqrt{1+W-n^2} = k\pi/2$, which are plotted in Figure 2. Nevertheless, only the bifurcations from the curves AB ($\Lambda\sqrt{1+W} = \pi$) and BC ($\Lambda\sqrt{W} = \pi/2$) are significant in practice (the curve ABC represents the transition from stable to unstable cylinders).

2. BIFURCATION TO EQUILIBRIUM SHAPES

Let $W = W_0(\Lambda)$ be the equation of any of the curves AB or BC, and \bar{F} be a nontrivial solution of Eqs. 5-6 for $W = W_0(\Lambda)$. For a fixed value of Λ , the variables u and q , and the parameters ϵ and b are introduced as

$$W = W_0 + b, \quad p = 1 - \frac{1}{2}W_0 - \frac{1}{2}b + q, \quad \bar{F} = 1 + \epsilon\bar{F}(\theta, z) + u(\theta, z)$$

Eqs. 1-4 may be written in the form

$$M(1 + \epsilon\bar{F} + u) + 1 + q + (W_0 + b)(2 + \epsilon\bar{F} + u)(\epsilon\bar{F} + u)/2 - Bz = 0 \quad (7)$$

$$u(\theta, \pm\Lambda) = 0, \quad u(\theta + 2\pi, z) = u(\theta, z), \quad \langle \epsilon\bar{F} + u, 2 + \epsilon\bar{F} + u \rangle = 0 \quad (8)$$

$$\langle \bar{F}, u \rangle = 0 \quad (9)$$

in terms of the inner product

$$\langle f, g \rangle = \int_{-\Lambda}^{\Lambda} dz \int_0^{2\pi} f g d\theta$$

Observe that condition (9) defines the parameter ϵ as

$$\epsilon = \langle \bar{F}, \bar{F} \rangle / \langle \bar{F}, \bar{F} \rangle$$

The problem 7-9 provides ϵ , $u(\theta, z)$ and q in terms of b and B . As $B, b \rightarrow 0$, such functions may be calculated by means of standard Perturbation Techniques (Refs. 8-9). However, a direct use of such techniques, (a) requires to anticipate certain properties of the solution and (b) leads to a singular perturbation problem in the case $B \neq 0$ (Ref. 9). Both difficulties are avoided by using the idea of bifurcation equation. We consider the auxiliary equation

$$M(1 + \epsilon\bar{F} + u) + 1 + q + (W_0 + b)(2 + \epsilon\bar{F} + u)(\epsilon\bar{F} + u)/2 - Bz + \psi\bar{F} = 0 \quad (10)$$

which is identical with Eq. 7 if $\psi = 0$. It may be shown that Eqs. 8-10 uniquely define

$$\psi = \psi(\epsilon, b, B)$$

$$u = u(\theta, z; \epsilon, b, B), \quad q = q(\epsilon, b, B) \quad (11)$$

at least as $\epsilon, b, B \rightarrow 0$ (Implicit Function Theorem). Such functions correspond to solutions of Eqs. 7-9 if and only if ϵ, b and B satisfy

$$\psi(\epsilon, b, B) = 0 \quad (12)$$

which is known as the bifurcation equation of the problem. If ϵ , b and B satisfy the bifurcation equation the functions 11 are solutions of Eqs. 7-9.

3. BIFURCATION EQUATION IN THE ABSENCE OF GRAVITY ($B=0$)

The Bond number, B , will vanish throughout this section. If, in addition, $\epsilon = 0$, Eqs. 8-10 have the so-

lution $\psi = q = 0$, $u \equiv 0$; since the solution of Eqs. 8-10 is unique,

$$\psi(0, b, 0) = 0, \quad u(\theta, z; 0, b, 0) \equiv 0, \quad q(0, b, 0) = 0$$

and

$$\psi(\epsilon, b, 0) = \epsilon g(\epsilon, b)$$

$$u(\theta, z; \epsilon, b, 0) = \epsilon v(\theta, z; \epsilon, b), \quad q(\epsilon, b, 0) = \epsilon r(\epsilon, b)$$

where g , v and r are C^∞ functions of ϵ and b ; their Taylor series expansions at $b = B = 0$ yield

$$\psi(\epsilon, b, 0) = \epsilon \sum g_{ij} \epsilon^i b^j, \quad u(\theta, z; \epsilon, b, 0) = \epsilon \sum v_{ij}(\theta, z) \epsilon^i b^j, \quad q(\epsilon, b, 0) = \epsilon \sum r_{ij} \epsilon^i b^j \quad (13)$$

When the expansions (13) are inserted into the equations 8-10, and the coefficient of each power $\epsilon^i b^j$ is set to zero, a recursive sequence of linear problems results, to calculate g_{ij} , v_{ij} and r_{ij} .

3.1 Axisymmetric case (Curve AB of Figure 2)

In this case

$$W_0(\Lambda) = (\pi/\Lambda)^2 - 1, \quad \bar{F} = \sin(\pi z/\Lambda)$$

Then

$$g_{00} = 0, \quad v_{00} \equiv 0, \quad r_{00} = 0; \quad g_{01} = -1$$

$$g_{10} = 0, \quad r_{10} = \frac{2-W_0}{4},$$

$$v_{10} = -\frac{W_0}{4(1+W_0)} \cos \frac{\pi z}{\Lambda} - \frac{1}{4} + \frac{1}{4(1+W_0)} \cos \frac{2\pi z}{\Lambda}$$

and

$$g_{20} = -\frac{3(1+W_0+W_0^2/2+W_0^3/4)}{2(1+W_0)} \quad (14)$$

Then, the bifurcation equation 12 yields

$$b \equiv W - W_0(\Lambda) = g_{20} \epsilon^2 + o(\epsilon^2) \quad (15)$$

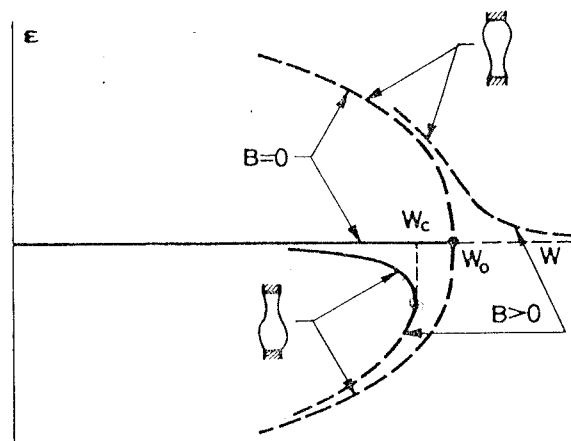


Figure 3. Axisymmetric bifurcation.

When b and ϵ satisfy Eq. 15

$$F(\theta, z) = 1 + \epsilon \sin(\pi z / \Lambda) + \epsilon^2 v_{10}(z) + o(\epsilon^2)$$

$$p = 1 - W_0 / 2 + \epsilon^2 r_{10} + o(\epsilon^2)$$

is a solution of Eqs. 1-4. Eq. 15 has been plotted in Figure 3, and g_{20} in terms of Λ , in Figure 4. Observe that the bifurcation is subcritical; then, the bifurcated solutions are expected to be unstable.

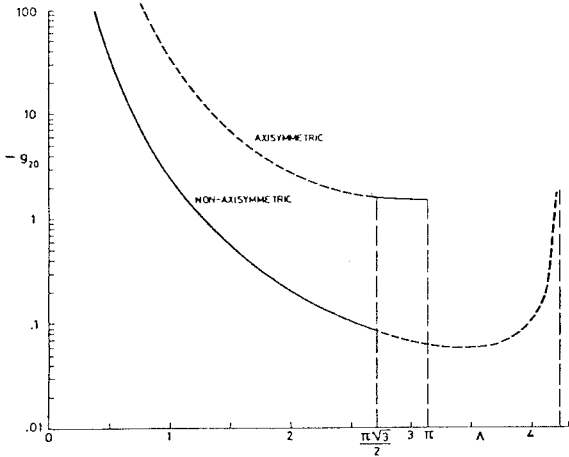


Figure 4. g_{20} vs. Λ for axisymmetric (upper curve) and non-axisymmetric (lower curve) bifurcation.

3.2 Non-axisymmetric case (Curve BC of Figure 2)

In this case

$$W_0(\Lambda) = (\pi / 2\Lambda)^2, \quad \bar{F} = \cos \theta \cos(\pi z / 2\Lambda) \quad (16)$$

Then

$$g_{00} = 0, \quad v_{00} = 0, \quad r_{00} = 0; \quad g_{01} = -1, \quad g_{10} = 0$$

$$r_{10} = -\frac{1+2W_0}{8} + \frac{1+W_0}{8(3W_0-1)} \frac{(3W_0-1)\sqrt{1+W_0}\Lambda + \tan(\sqrt{1+W_0}\Lambda)}{\sqrt{1+W_0}\Lambda - \tan(\sqrt{1+W_0}\Lambda)}$$

$$v_{10} = -\frac{1+2W_0+8r_{10}}{8(1+W_0)} \left[1 - \frac{\cos(\sqrt{1+W_0}z)}{\cos(\sqrt{1+W_0}\Lambda)} \right] + \frac{1}{8(3W_0-1)} \left[\cos \frac{\pi z}{\Lambda} + \frac{\cos(\sqrt{1+W_0}z)}{\cos(\sqrt{1+W_0}\Lambda)} \right] + \frac{3+2W_0}{8(3-W_0)} \left[1 - \frac{\cos(\sqrt{W_0-3}z)}{\cos(\sqrt{W_0-3}\Lambda)} \right] \cos 2\theta + \left[\cos \frac{\pi z}{\Lambda} + \frac{\cos(\sqrt{W_0-3}z)}{\cos(\sqrt{W_0-3}\Lambda)} \right] \frac{\cos 2\theta}{8(1+W_0)}$$

and

$$g_{20} = \frac{18-7W_0-9W_0^2}{32} - \frac{(2+W_0)(9+4W_0)}{32(1+W_0)} + \frac{9W_0(1+W_0)}{8(3W_0-1)} \left[\frac{(1+2W_0)^2}{2} - \frac{W_0\sqrt{1+W_0}\Lambda}{\sqrt{1+W_0}\Lambda - \tan(\sqrt{1+W_0}\Lambda)} \right] - \frac{W_0(3+W_0)}{4(1+W_0)(3-W_0)} \left[\frac{3+2W_0}{2} - \frac{W_0(3+W_0)}{1+W_0} \frac{\tan(\sqrt{W_0-3}\Lambda)}{\sqrt{W_0-3}\Lambda} \right] \quad (17)$$

The bifurcation equation 12 leads to

$$b \equiv W - W_0(\Lambda) = g_{20}\epsilon^2 + o(\epsilon^2) \quad (18)$$

If b and ϵ satisfy Eq. 18

$$F(\theta, z) = 1 + \epsilon \cos \theta \cos(\pi z / 2\Lambda) + \epsilon^2 v_{10} + \dots$$

$$p = 1 - W_0 / 2 + \epsilon^2 r_{10} + \dots$$

is a solution of Eqs. 1-4. Again, Eq. 18 is plotted in Figure 5, and g_{20} vs. Λ , in Figure 4.

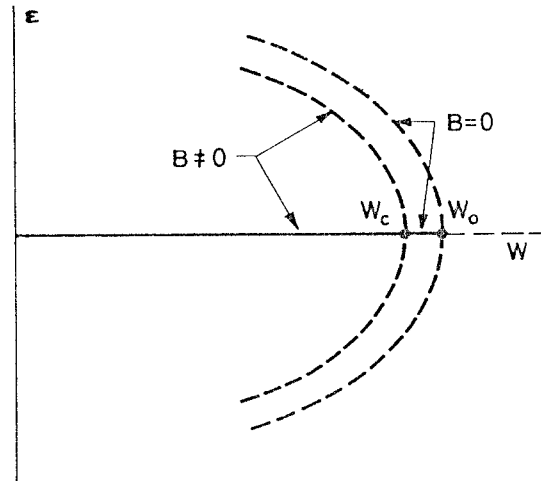


Figure 5. Non-axisymmetric bifurcation.

The area of a section $z = \text{const.}$ of the liquid bridge is

$$A(z) = \frac{1}{2} \int_0^{2\pi} F^2 d\theta = \frac{\pi \epsilon^2}{2} \left[-\frac{W_0+8r_{10}}{1+W_0} + \frac{3W_0}{3W_0-1} \cos \frac{\pi z}{\Lambda} + \frac{1+W_0+(3W_0-1)(1+2W_0+8r_{10})}{(1+W_0)(3W_0-1)} \frac{\cos(\sqrt{1+W_0}z)}{\cos(\sqrt{1+W_0}\Lambda)} \right] + \dots$$

$A(z)$ is seen to have a maximum at $z = 0$, and two minima, at $z = \pm |z_{\min}|$. At first approximation of A_{\max} , A_{\min} and $|z_{\min}|$ are given in Figure 6.

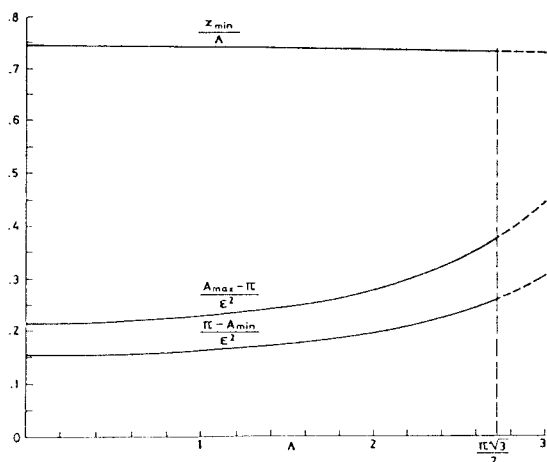


Figure 6. A_{\max} , A_{\min} , $|z_{\min}|$ vs. A for non-axisymmetric bifurcated liquid bridges.

4. EFFECT OF A RESIDUAL GRAVITY

4.1 Axisymmetric case

As $\epsilon, b, B \rightarrow 0$

$$\psi(\epsilon, b, B) = \psi(\epsilon, b, 0) + \psi_1 B + \dots \quad (19)$$

$$u(z; \epsilon, b, B) = u(z; \epsilon, b, 0) + u_1(z)B + \dots \quad (20)$$

$$q(\epsilon, b, B) = q(\epsilon, b, 0) + q_1 B + \dots \quad (21)$$

where $\psi(\epsilon, b, 0)$, $u(z; \epsilon, b, 0)$ and $q(\epsilon, b, 0)$ has been calculated in section 3. ψ_1 , u_1 and q_1 are calculated from the linear problem obtained by inserting Eqs. 19-21 into Eqs. 8-10, and setting to zero the coefficient of B ,

$$\psi_1 = \frac{2}{\sqrt{1+W_0}}, \quad q_1 = 0, \quad u_1 = z[1 + \cos(\sqrt{1+W_0}z)]/\sqrt{1+W_0}$$

The resulting bifurcation equation is

$$\epsilon(-b + g_{20}\epsilon^2 + \dots) + 2B/\sqrt{1+W_0} + \dots = 0 \quad (22)$$

For $B = \text{constant}$, the curves $\epsilon-b$ given by Eq. 22 are as those plotted in Figure 3. In particular, the new stability limit is found to be

$$b_c \equiv W_c - W_0(A) = 3[g_{20}B^2/(1+W_0)]^{1/3} + \dots$$

4.2 Non-axisymmetric case

The equations 8-10 (W_0 and \bar{F} as given by Eq. 16) are invariant under the symmetries

$$\theta \rightarrow \theta + \pi, \quad \epsilon \rightarrow -\epsilon, \quad \psi \rightarrow -\psi$$

and

$$z \rightarrow -z, \quad B \rightarrow -B$$

Since the solution of Eqs. 8-10 is unique, these symmetries lead to

$$\psi(-\epsilon, b, B) \equiv -\psi(\epsilon, b, B), \quad \psi(\epsilon, b, -B) \equiv \psi(\epsilon, b, B)$$

As a consequence, ψ is an even function of B , and it is an odd function of ϵ ; therefore, it may be written in the form $\psi(\epsilon, b, B) = \epsilon\phi(\epsilon^2, b, B^2)$, where ϕ is a C^∞ function of ϵ^2 , b and B^2 , and the bifurcation equation is

$$\epsilon(-b + g_{20}\epsilon^2 + a_1B^2 + \dots) = 0$$

It provides a relation between ϵ and b (for a fixed value of B) as that sketched in Figure 5. The stability limit is

$$b_c \equiv W_c - W_0(A) = a_1B^2 + \dots$$

a_1 , which is expected to be negative, could be calculated from a (too ugly to deal with) system of recursive linear problems.

5. RESULTS AND CONCLUSIONS

The analysis of sections 2-4 was made for a fixed value of A . Bifurcation equations, for a fixed Weber number W , are now easily obtained.

- Axisymmetric case

The bifurcation equation is

$$\epsilon[-2(1+W)l + g_{20}\epsilon^2 + \dots] + 2B/\sqrt{1+W} + \dots = 0$$

where

$$A = A_0(W)(1+l), \quad A_0(W) = \pi/\sqrt{1+W}$$

and g_{20} is obtained by a substitution of W_0 by W in Eq. 14. The stability limit is

$$l_c \equiv \frac{A_c - A_0(W)}{A_0(W)} = \frac{3}{4} [g_{20}B^2/(1+W)^4]^{1/3} + \dots$$

For $W = 0$ (no rotation), $g_{20} = -3/2$, $A_0 = \pi$ and

$$A_c = \pi[1 - \frac{3}{2}(\frac{3}{2}B^2)^{1/3} + \dots] \quad (23)$$

The estimate $A_c = \pi/\sqrt{1+B}$, which was obtained in Ref. 10, has been used sometimes in the Literature. Observe that it is not asymptotically correct, as $B \rightarrow 0$. A comparison of the approximation of Eq. 23 with numerical and experimental values (taken from Ref. 11) is given in Figure 7.

- Non-axisymmetric case

The bifurcation equation is

$$\epsilon[-2Wl + g_{20}\epsilon^2 + a_1B^2 + \dots] = 0$$

where

$$A = A_0(W)(1+l), \quad A_0(W) = \pi/\sqrt{4W}$$

and g_{20} is obtained by substitution of W_0 by W in Eq. 17.

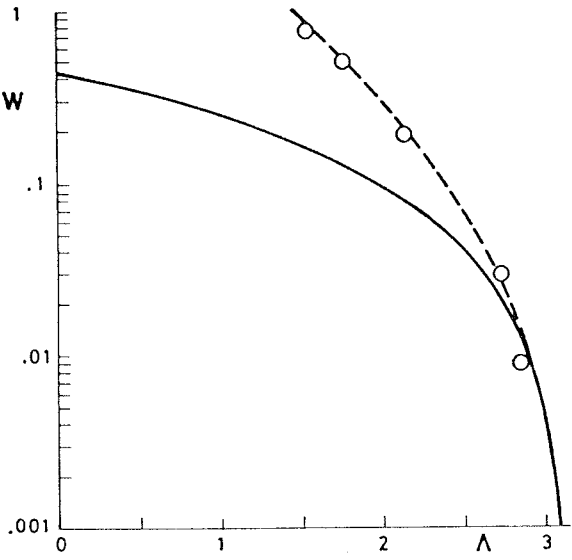


Figure 7. The stability limit vs. the Bond number for $W = 0$: (---) numerical, (—) as given by Eq. 23, and (o) experimental.

Some comments about the results obtained above are in order:

- In the segment AB of Figure 2, $W \leq 1/3$ and $g_{20} \approx -3/2$ (see Figure 4). Therefore, the stability limit is
$$\Lambda_c \approx \frac{\pi}{\sqrt{1+W}} \left\{ 1 - \frac{3}{2} \left[\frac{3B^2}{2(1+W)} \right]^{1/3} + \dots \right\}$$
- In part of the segment BC, $|g_{20}|$ is quite small (see Figure 4). Therefore, the size of the perturbations leading to breakage of the bridge is expected to be large in the non-axisymmetric case, as compared with that of the axisymmetric case.
- In a dynamic analysis of the liquid bridge, the mode $F-1 = eF$, which loses stability as (Λ, W) passes through the curve ABC in Figure 2, is expected to be decoupled, in first approximation, from the remaining oscillating modes. Then, at least in a first stage of a purely non-axisymmetric breakage process, the liquid bridge is expected to be as the bifurcated shapes which were obtained in 3.2, with a central paunch and two symmetric necks.
- The curve AB is much more sensitive than the curve BC to a residual gravitational effect.

REFERENCES

1. Gillis J 1961, Stability of a column of rotating viscous liquid, *Proc. Camb. Phil. Soc.*, 57, 152-159.
2. Hardy S & Corriel S R 1974, Melt shape in weightless crystal growth, *NBS Space Processing Research*, NBSIR 74-611, US Department of Commerce.
3. Fowle A A et al. 1976, *Float-zone processing in a weightless environment*, NASA CR-2768.
4. Martínez I 1978, *Hidrostatica de la zona flotante*, Tesis Doctoral, Universidad Politécnica de Madrid.
5. Brown R A & Scriven L E 1980, The shapes and stability of captive rotating drops, *Phil. Trans. R. Soc. London*, 297, 51-79.
6. Struik D J 1957, *Classical Differential Geometry*, Addison Wesley.
7. Lang S 1969, *Real Analysis*, Addison Wesley.
8. Millman M H & Keller J B 1969, Perturbation theory of nonlinear boundary-value problems, *J. Math. Phys.*, 10, 342-361.
9. Matkowsky B J & Reiss E I 1977, Singular perturbations of bifurcations, *SIAM J. Appl. Math.* 33(2), 230-255.
10. Carruthers J R & Grasso M 1972, Studies of Flotating liquid zones in simulated zero gravity, *J. Appl. Phys.* 43(2), 436-445.
11. Corriel et al. 1977, Stability of liquid zones, *J. Colloid Interface*, 60, 126-136.